



POLİTEKNİK DERGİSİ

*JOURNAL of POLYTECHNIC*

ISSN: 1302-0900 (PRINT), ISSN: 2147-9429 (ONLINE)

URL: <http://dergipark.org.tr/politeknik>



# Effect of SiC particle size on the microstructural, mechanical and oxidation properties of In-situ synthesized HfB<sub>2</sub>-SiC composites

*SiC partikül boyutunun yerinde sentezleme yöntemi ile üretilen HfB<sub>2</sub>-SiC kompozitlerinin mikroyapısal, mekanik ve oksidasyon özellikleri üzerine etkisi*

*Yazar(lar) (Author(s)): Kübra GÜRCAN<sup>1</sup>, Bora DERİN<sup>2</sup>, Erhan AYAS<sup>3</sup>*

*ORCID<sup>1</sup>: 0000-0003-0434-1518*

*ORCID<sup>2</sup>: 0000-0002-2472-4535*

*ORCID<sup>3</sup>: 0000-0003-0592-3990*

**Bu makaleye şu şekilde atıfta bulunabilirsiniz(To cite to this article):** Gürcan K., Derin B. and Ayas E. "Effect of SiC particle size on the microstructural, mechanical and oxidation properties of in-situ synthesized HfB<sub>2</sub>-SiC composites", *Politeknik Dergisi*, 24(2): 503-510, (2021).

**Erişim linki (To link to this article):** <http://dergipark.org.tr/politeknik/archive>

**DOI:** 10.2339/politeknik.682256

# Effect of SiC Particle Size on The Microstructural, Mechanical And Oxidation Properties of In-Situ Synthesized HfB<sub>2</sub>-SiC Composites

## Highlights

- ❖ Production of HfB<sub>2</sub>-SiC composites was carried out by the spark plasma sintering (SPS) method using HfO<sub>2</sub>, B, and SiC as starting powders.

## Graphical Abstract

In-situ synthesis and densification of HfB<sub>2</sub>-SiC ceramic composites were studied by the spark plasma sintering (SPS) method using HfO<sub>2</sub>, B, and SiC as starting powders.

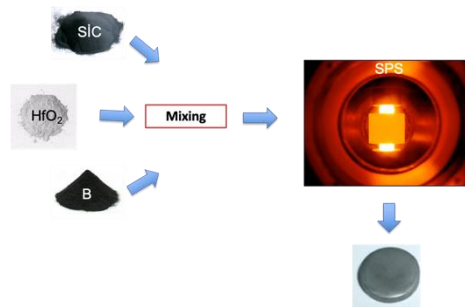


Figure 1. Graphical abstract

## Aim

Production of HfB<sub>2</sub>-20 vol% SiC composites by using HfO<sub>2</sub>, B and SiC starting powders by SPS method under predetermined conditions.

## Design & Methodology

Powders were mixed in a planetary ball mill, and the sintering process was carried out in SPS furnace.

## Originality

Different from the literature, our study mainly contains with both synthesis and densification of HfB<sub>2</sub>-SiC ceramics in two step SPS process. Another difference is that as starting powders we introduced HfO<sub>2</sub> elemental B and two different SiC powders

## Findings and Conclusions

The formation of the HfB<sub>2</sub> was completed at 1000 ° C and the HfB<sub>2</sub>-SiC composite was formed. This composite is stable up to 1810 ° C.

Fine SiC and higher sintering temperature provided higher densification, mechanical properties and oxidation resistance.

## Declaration of Ethical Standards

The authors of this article declare that the materials and methods used in this study do not require ethical committee permission and/or legal-special permission.

# SiC Partikül Boyutunun Yerinde Sentezleme Yöntemi ile Üretilen HfB<sub>2</sub>-SiC Kompozitlerinin Mikroyapısal, Mekanik ve Oksidasyon Özellikleri Üzerine Etkisi

*Araştırma Makalesi / Research Article*

**Kübra GÜRCAN<sup>1\*</sup>, Bora DERİN<sup>2</sup>, Erhan AYAS<sup>1</sup>**

<sup>1</sup>Mühendislik Fakültesi, Malzeme Bilimi ve Mühendisliği Bölümü, Eskişehir Teknik Üniversitesi, Türkiye

<sup>2</sup>Kimya ve Metalurji Fakültesi, Metalurji ve Malzeme Mühendisliği Bölümü, İstanbul Teknik Üniversitesi, Türkiye

(Geliş/Received : 30.01.2020 ; Kabul/Accepted : 20.04.2020)

## ÖZ

Hafniyum diborür-silisyum karbür (HfB<sub>2</sub>-SiC) seramik kompozitlerinin sentezlemesi ve yoğunlaştırılması, başlangıç tozları olarak HfO<sub>2</sub>, B ve SiC kullanılarak spark plazma sinterleme (SPS) yöntemi ile incelenmiştir. SiC partikül boyutunun (~2µm ve ~10µm) üretilen kompozitlerin mekanik özellikleri ve oksidasyon direncine etkisi kapsamlı olarak araştırılmıştır. Elde edilen sonuçlara göre ince SiC partikül takviyesi ile en yüksek yoğunluk (~95 TY) elde edilmiştir. İnce SiC içeren kompozitlerin ölçülen Vickers sertliği ve kırılma tokluğu sırasıyla 14.3 GPa ve 5.42 MPa.m<sup>1/2</sup> olarak hesaplanmıştır. Kırılma türü tane içi halden tane sınırları şekline değişmiş olup, toklaştırma mekanizması olarak çatlak saptırmanın aktif olduğu gözlenmiştir. Oksidasyon testi sonucundan, ince SiC partiküllerine sahip kompozit yapının kaba SiC içeren kompozit yapıya kıyasla homojen olmayan oksit tabakası içerdiği gözlemlenmiştir.

**Anahtar Kelimeler:** Aşırı yüksek sıcaklık seramikleri, HfB<sub>2</sub>-SiC, yerinde sentezleme, SPS.

## Effect of SiC Particle Size on the Microstructural, Mechanical and Oxidation Properties of In-situ Synthesized HfB<sub>2</sub>-SiC Composites

### ABSTRACT

In-situ synthesis and densification of hafnium diboride - silicon carbide (HfB<sub>2</sub>-SiC) ceramic composites were studied by the spark plasma sintering (SPS) method using HfO<sub>2</sub>, B, and SiC as starting powders. Influence of SiC particle size (~2 µm and ~10 µm) on mechanical properties and oxidation resistance of in-situ composites were extensively investigated. According to the achieved results, the highest densification (~95 % TD) was obtained with fine SiC particle reinforcement. The measured Vickers hardness and fracture toughness of the composites containing fine SiC were 14.3 GPa and 5.42 MPa.m<sup>1/2</sup>, respectively. The fracture mode changed from transgranular cleavage to a mixed-mode, and the crack deflection was believed to be the primary toughening mechanism. From oxidation test result, the composite with fine SiC particles exhibited more inhomogeneous oxide scales compared to that of coarse SiC containing composite.

**Keywords:** Ultra high temperature ceramics, HfB<sub>2</sub>-SiC, in-situ synthesis, SPS.

### 1. INTRODUCTION

The development of hypersonic-atmospheric re-entry vehicles and nuclear facilities increased the demand for materials that are resistant to extremely high temperatures and oxidizing environments. Ultra-High Temperature Ceramics (UHTC) based on transition metal borides meet above-mentioned requirements due to their high melting temperature and good thermo-physical properties. Nowadays, HfB<sub>2</sub> attracts more attention among the researchers than other UHTC members due to its high thermal conductivity and chemical stability [1-3]. A number of studies were reported on the synthesis or synthesis/densification of micron and nano-sized HfB<sub>2</sub>

powders by using solid-state carbothermal/borothermal reduction, mechanical alloying, self-propagation high-

temperature synthesis (SHS), pressureless sintering, spark plasma sintering (SPS), and hot pressing (HP) methods [4-9]. However, high covalent bonding, low self-diffusion coefficient, as well as the presence of oxide impurities limit full densification of monolithic HfB<sub>2</sub> using the above-mentioned techniques.

HfB<sub>2</sub> oxidation preferentially occurs at low temperatures (<1000°C) according to the reaction (1). The oxide scale provides an effective barrier to oxygen diffusion up to 1100°C owing to the filling of pores with molten B<sub>2</sub>O<sub>3</sub> [10]. However, oxidation of HfB<sub>2</sub> starts around 1400 °C resulting from the rapid evaporation of B<sub>2</sub>O<sub>3</sub> due to its high vapor pressure.



Some earlier studies [11-17] focused on improvement of oxidation resistance of these ceramics showed that the presence of SiC ranging from 10 to 30 vol% was required

\*Sorumlu Yazar (Corresponding Author)  
e-posta : kubragurcan@eskisehir.edu.tr

for achieving high oxidation resistance at elevated temperatures. Presence of SiC in HfB<sub>2</sub> ceramics led to reduction of their oxidation rates by the formation of protective glassy borosilicate scale in the oxidizing conditions. This glass layer was found to be protective against non-air flowing atmosphere up to 2000°C. The studies showed that SiC addition also improved microstructural and mechanical properties of HfB<sub>2</sub> ceramics at high temperatures.

Spark Plasma Sintering is one of the most preferred methods of sintering such highly covalent bonded materials. The full or nearly full-density consolidation, low sintering temperature, very short sintering time, and products with improved mechanical and thermal properties were the main advantages of the process [18]. Similar to SPS, reactive spark plasma sintering (R-SPS) also allows simultaneous synthesis and sintering in single process step, when appropriate reactants were used. Up to now, sintering temperature, sintering techniques and effect of SiC amount in matrix have been extensively investigated [19-25], whereas there are limited in-situ synthesis studies that discuss the oxidation behavior of UHTC-SiC composites [26, 27].

For that reason, present study focuses on the production and investigation of mechanical and oxidation properties of HfB<sub>2</sub>-20 vol% SiC composites by using HfO<sub>2</sub>, B and SiC starting powders by SPS method under predetermined conditions. The scope of present study includes; (i) estimation of possible reaction products by using FactSage thermochemical modeling software [28]; (ii) comparison of the effect of different SiC particle size on microstructural, mechanical and oxidation features of the composites.

## 2. MATERIALS AND METHOD

### 2.1. Powder preparation and SPS process

Commercially available HfO<sub>2</sub> (ABCR-GmbH, Germany, d<sub>50</sub>: 1 µm), B (Pavezyum Inc., Turkey, d<sub>50</sub>: 200 nm) and two different SiC (UF05, HC Starck-Germany, d<sub>50</sub>: 1.4 µm and Saint Gobain-France, d<sub>50</sub>: 12 µm) powders were selected as starting powders. Calculated weight percent and molar amount of starting powders were given in Table 1 on the basis of targeting 20 vol% SiC of HfB<sub>2</sub>-SiC composite.

**Table 1.** Calculated weight percent and molar amount of starting powders

Starting Powders	HfO <sub>2</sub>	B	SiC
weight %	79,67	13,66	6,67
molar amount	0,37	1,26	0,17

Powders were mixed in a planetary type ball mill (Pulverisette, P6, Fritsch) in 2-propanol using Si<sub>3</sub>N<sub>4</sub> grinding media at 450 rpm for 90 min and dried in a rotary evaporator at 60°C. To break up agglomerates; the powders were sieved under 250 µm. In-situ synthesis of HfB<sub>2</sub>-SiC composites was utilized under the vacuum atmosphere in an SPS furnace (HPD- 50, FCT GmbH,

Germany). The powders were put into a graphite die 20 mm in diameter and a graphite foil coated with h-BN particles was incorporated to prevent reaction between graphite die and the powders. Temperature was increased with a controlled electric current and measured on the graphite die surface with an optical pyrometer. To minimize the heat loss, graphite die surface was covered with a graphite blanket 2 mm in thickness. A two-step heating profile was designed regarding the thermochemical data obtained from the “Equilib” module of FactSage 7.1 by predicting the possible reaction products combined with the displacement data obtained from the SPS software. All gas, liquid and the stoichiometric solid phases were selected from the FactPS database. Temperature was raised up to 1000°C and kept constant for 10 min in order to promote borothermal reduction of HfO<sub>2</sub> under 15 MPa uniaxial pressure. Then temperature was further raised up to final sintering temperatures which were selected as 1950°C. The specimens were held at the maximum sintering temperature for 30 min under 50 MPa uniaxial pressure.

### 2.2. Material characterisation

The bulk densities of sintered samples were determined by using the Archimedes method based on theoretical density of HfB<sub>2</sub> (11.2 g/cm<sup>3</sup>) and SiC (3.2 g/cm<sup>3</sup>) after removing surface layer of graphite by grinding. For X-Ray Diffraction (XRD) analysis samples were crushed and milled under 63 µm particle size. Qualitative phase analysis was accomplished by using an X-Ray diffractometer (Rigaku Rint2200 series) at a scan speed of 1°/min. Polished surfaces of samples were examined by using a scanning electron microscope (Supra 50 VP, Zeiss-Germany) equipped with an EDX detector (Oxford Instruments, UK). The Vickers hardness (Hv10) from the polished surfaces of the sintered samples was measured by using an indenter (EMCOTest, M1C-Germany) under a load of 10 kg applied for 5 sec. At least five indentations were applied for each sample. The fracture toughness (K<sub>IC</sub>) of the samples was evaluated from radial cracks formed during the indentation test [29].

### 2.3. Oxidation analysis

Tests were carried out on samples in dry air at temperature of 1650°C for 1h in a bottom-loading furnace. Rectangular bars with dimensions of 10 mm x 4 mm x 4mm were sliced from SPS pellets and mechanically polished up to 1 µm diamond finish. Oxide scales formed on samples after isothermal oxidation tests were examined by SEM and EDX. Oxide scale thicknesses were averaged out of measurements from about 5 different locations.

## 3. RESULTS AND DISCUSSIONS

### 3.1. Thermodynamical, phase and microstructural evaluation

Samples were designated as HSc and HSf, respectively which ‘c’ and ‘f’ corresponds to the particle size of SiC powders (coarse and fine). SEM (BSE) images depicting

the microstructures of HSc and HSf were given in Figure 1.a and Figure 1.b., respectively. A uniform distribution of the constituent phases with formed HfB<sub>2</sub> phase appearing brighter than SiC due to lower atomic number of the latter phase. Identification of phases in these images has been based on qualitative confirmation of composition by EDX analysis. It was clearly observed that, HSf has denser microstructure despite observed porosities for both samples. As a matter of fact, the relative density values of HSc and HSf measured by Archimedes were calculated as 90% and 95%, respectively.

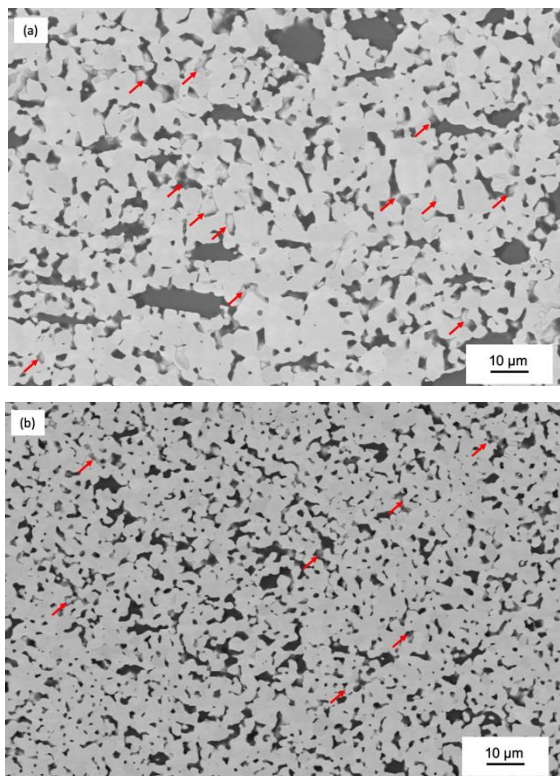


**Figure 1.** SEM (BSE) images taken from the polished surface of the a)HSc and b)HSf

Calculated densities and SEM images confirmed that density of the samples prepared by using finer SiC was much higher than the samples prepared by using coarser SiC. The average particle size of HfB<sub>2</sub> calculated from the SEM images was  $\sim 2 \mu\text{m}$  for HSf and  $\sim 10 \mu\text{m}$  for HSc, respectively. It was clearly observed that, size of HfB<sub>2</sub> grains was directly related with the initial size of SiC particles in the final microstructure. Some pull out defects were also observed in both microstructures (shown with red arrows). It is well known that applied uniaxial pressure, high heating and cooling rate induce internal residual stress during SPS due to the thermal anisotropy, thermal stresses are developed within the composite microstructure during cooling [7, 22, 26, 30, 31]. With the addition of SiC, tensile stresses develop at the HfB<sub>2</sub> grains while compressive stresses develop with in the SiC particles due to the difference of thermal

expansion coefficient between HfB<sub>2</sub> ( $\alpha = 6.3 \cdot 10^{-6} \text{ K}^{-1}$ ) [2] and SiC ( $\alpha = 4.7 \cdot 10^{-6} \text{ K}^{-1}$ ) [32]. Consequently, high residual stresses which come up at the HfB<sub>2</sub>-SiC interfaces is resulted the microstructural defects. These type of defects induced by high residual stresses for HfB<sub>2</sub> based composites have been confirmed by many studies [7, 22, 26].

It was clearly observed that the average particle size of starting SiC powder has a significant effect in controlling the final microstructure of samples, including managing HfB<sub>2</sub> grain size. In Figure 1.a microstructure containing smaller grains were obtained by using fine SiC particles for in-situ synthesized and sintered HfB<sub>2</sub>-SiC composites. Also, these results were in accordance with that grain growth was inhibited with SiC addition in ZrB<sub>2</sub> and TiB<sub>2</sub> ceramics due to the pinning effect [33, 34].

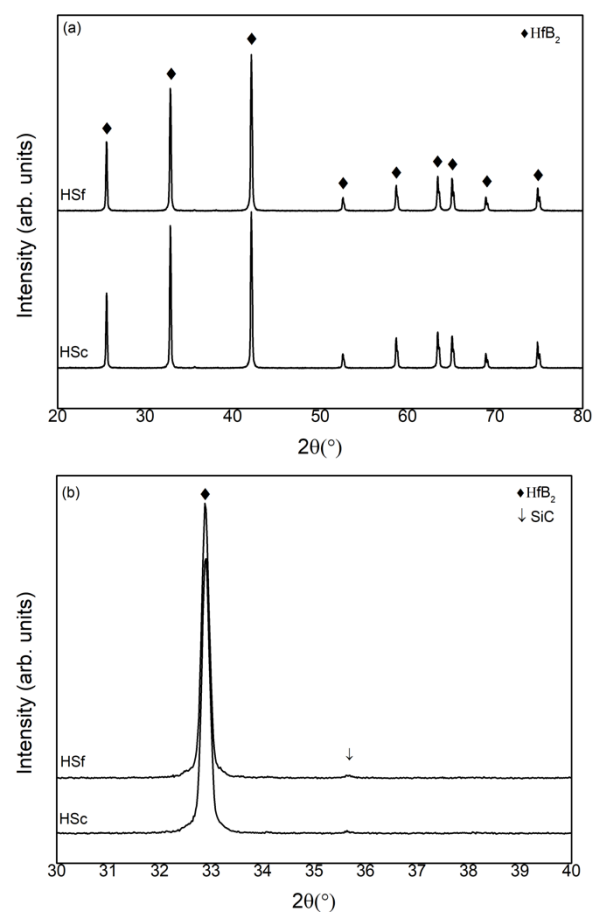


**Figure 2.** a)Comparative XRD patterns of HSc and HSf b) magnified view at 30-40° 2θ angle range.

XRD patterns of the samples HSc and HSf were given in Figure 2.a. HfB<sub>2</sub> (ICDD 38-1398) was detected as the only crystalline phase. The patterns of the SiC phases were not distinguishable due to the very small quantities based on the mass ratio of SiC in the total mass amount. For that reason, between 30-40° 2θ angle range low speed XRD analysis was conducted in Figure 2.b. The minor

patterns of SiC phase were observed at the specified  $2\theta$  angle range. Another remarkable point in the XRD patterns was observation of the peaks with lower intensity at the right side of the main peaks, especially for the peaks  $2\theta > 55^\circ$ . It has been interpreted that these small peaks formed belong to non-stoichiometric hafnium boride phases ( $Hf_xB_y$ ) caused by the addition of excess amount of B and/or C in borothermal/boro-carbothermal reduction. Formation of the same peaks has also observed at the study of Ni et al [7]. This result was confirmed in the many study[35, 36].

Although the use of three different powder mixtures as starting powders obviously caused many complex reactions, no other peaks were observed beyond  $HfB_2$  and SiC. Figure 3.a. illustrates FactSage graph of the molar amount of variations of the with respect to temperature up to  $2000^\circ C$  under a vacuum of  $10^{-2}$  mbar. Molar ratios were taken as 0.377 mol  $HfB_2$  and 0.17 mol SiC, assuming that whole  $HfO_2$  transformed to  $HfB_2$ .

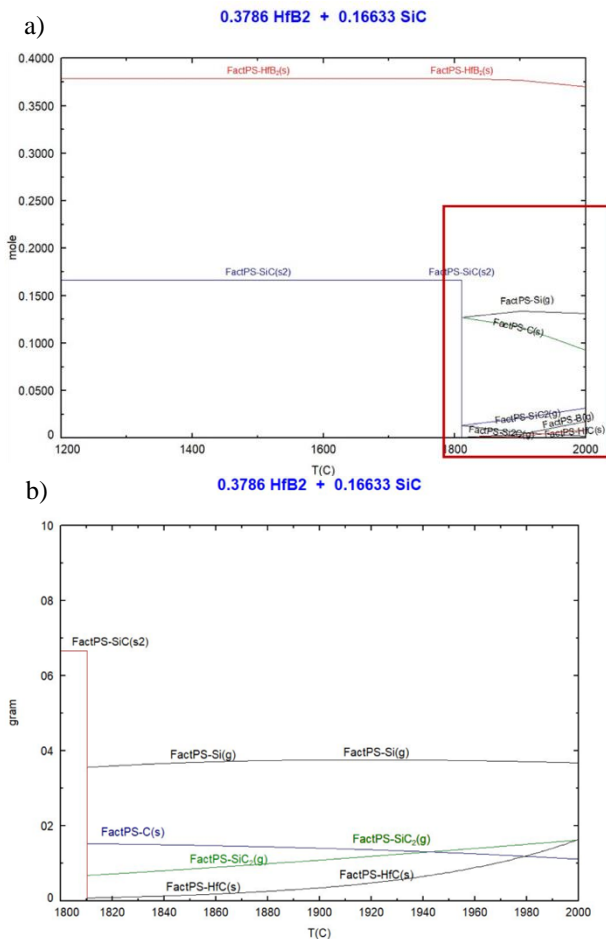


**Figure 3.** a) FactSage graph of the molar amount of variations of the with respect to temperature up to  $2000^\circ C$  b) magnified view of rectangular region under a vacuum of  $10^{-2}$  mbar.

According to the thermodynamically predictions, formed  $HfB_2$  and starting SiC phases were stable up to around  $1810^\circ C$ . Then, SiC was sharply consumed above  $1810^\circ C$  and  $Si(g)$ ,  $C(s)$ ,  $SiC(g)$  and  $Si_2C(g)$  formations were

occurred. (clear in magnified view of Figure 3.b). This result can be supported with calculated volume percent of samples with using Scandium Software, which was 9.6%, and 8.56% for HSc and HSf, respectively. Considering these ratios, dissociation of SiC was observed during the formation of composite. This result was also consistent with the literature, that silicon carbide did not melt when heated to elevated temperatures rather, it sublimates and/or dissociates under atmospheric pressure[37-39]. Another observation was the increasing of  $HfC(s)$  and  $B(g)$  contents at higher temperatures which could be explained by the replacement of carbon by boron in  $HfB_2$  phase. However, similar with the XRD results, no other phases than  $HfB_2$  and SiC were observed in the SEM images. Especially, possible formations of Si, C and  $HfC$  according to the thermodynamical predictions, were not detected. This result can be explained with (i) formation of these phases require longer times along with higher temperature and (ii) amount of these phases cannot be detectable with used technique. Figure 3.b. which was the magnified views of selected locations as insets of Figure 3.a. indicated that weight amount of Si, C and  $HfC$  increases with the increasing of temperature up to  $2000^\circ C$ . Despite their increasing amount these phases, their maximum amount was calculated as 4 gr from the FactSage (Fig. 3.b) based on the starting molar ratio. This amount is very low for detection in the present analysis techniques.

Notwithstanding these results gave a general information about the system, several processing-related parameters including uniaxially pressure, heating rate might cause alteration of reaction kinetics before the thermodynamically results. Nevertheless; a more detailed study was still required to understand the role of pressure in reaction kinetics of these kind of systems. It was well known that uniaxial pressure has a direct effect on particle re-arrangement and hence decrease the reaction and/or sintering temperature. In addition, particle size was associated with the driving force which was contribution of the pressure. In this study, increase in pressure and contribution of finer SiC particle size increased the reaction formation kinetics before the thermodynamically conditions. Also,  $HfB_2$  degradation and formation of  $HfC$  may be related with the applied pressure along with temperature. Indeed, such pressure effect on the formation of reactions during the pressure assisted formations have been also observed on different studies [30, 40-42].

**Table 2.** Measured hardness and the indentation fracture toughness of the samples

Sample Name	Hardness-Hv10 (GPa)	Fracture Toughness ( $MPa.m^{1/2}$ )
HSc	$13.22 \pm 0.22$	$3.84 \pm 0.21$
HSf	$14.3 \pm 0.31$	$5.42 \pm 1.09$

### 3.2. Mechanical properties

Measured hardness and the indentation fracture toughness of samples were summarized in Table 2.

The microhardness values of HSc and HSf were calculated as 13.2 and 14.3 GPa, respectively, which were quietly lower than the previous studies [33, 43, 44]. Both grain size and relative density could affect the microhardness. The increasing microhardness values for a decreasing SiC particle size could be a result of decreasing grain boundary dislocation frequencies and being intrinsic higher stress values for deformation to occur. Additionally, relative density also affects microhardness of materials directly. When pores were observed in the ceramic microstructures, lower microhardness values were obtained due to the absence of any resistance under the applied stresses of the pores, as expected.

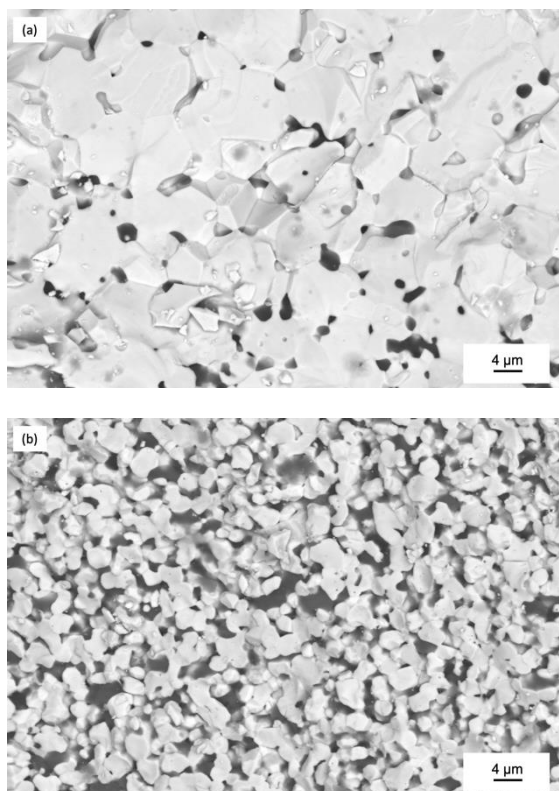


**Figure 4.** SEM(SE) images obtained from the fracture surfaces of the a)HSc and b)HSf

The fracture toughness values of the HSc and HSf were calculated as 3.84 to 5.42 MPa.m<sup>1/2</sup> respectively, which were quite similar with the previous studies [44]. The microhardness and fracture toughness were converse features to each other, as it was mainly accepted. However, the fracture toughness of the HSf sample was substantially higher than that of HSc sample due to the presence of microstructural defects like pull-out and porosity. SEM (SE) images obtained from the fracture surfaces of the HSc and HSf were illustrated in Figure 4.a and 4.b, respectively. For the sample HSc, transgranular crack propagation has been observed and this result explains low fracture toughness value (3.84 MPa.m<sup>1/2</sup>). However, HSf sample have exhibited a mixed fracture mode from transgranular to transgranular/intergranular

fracture. This formation led to achieve higher fracture toughness value (5.42 MPa.m<sup>1/2</sup>). Comparative crack paths induced during the Vickers indentation of HSf1950 were given in Figure 5. It indicated that crack deflection of the SiC particles was also an important mechanism. Because of the weak bonding of both HfB<sub>2</sub>-HfB<sub>2</sub> and HfB<sub>2</sub>-SiC grains, fracture toughness of composites has enhanced due to energy dissipation during the fracture of ceramics [45, 46].

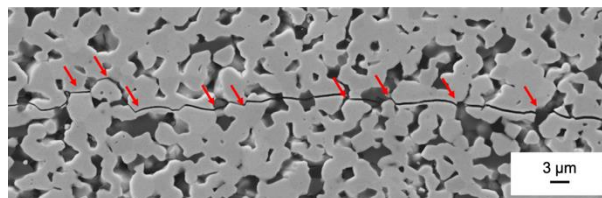


**Figure 5.** Crack paths induced during the Vickers indentation of HSf1950

### 3.3. Oxidation tests

The oxidation reactions and products for both HSc and HSf have been analyzed to understand their oxidation mechanisms. SEM images of the cross section of oxide scale formed on HSc and HSf by exposure at 1650°C for 1h were shown in Figure 6.a., and 6.b., respectively.

Magnified views of the selected locations which were shown with red rectangular in these images were shown in Figure 6.c., and 6.d., respectively. A SiO<sub>2</sub>-rich layer was occurred at the top and then followed by SiC-depleted layer which containing a mixture of SiO<sub>2</sub> and HfO<sub>2</sub> according to the EDX analysis. Comparison of these oxide scales for both samples in magnified images, SiO<sub>2</sub>-rich layer for HSc was made of a more continuous and smoother than HSf sample. Also, oxide scales for both samples appear porous with the average pore size and amount seems higher for HSf sample. The relatively rough regions with the higher magnifications in Figure 6.c., and 6.d., have been found by EDX analysis as HfO<sub>2</sub>-SiO<sub>2</sub>. Cracks and discontinuities were clearly visible in these locations of the oxide scale. In contrast to study of Hu et al. [47] oxide scales of sample containing of coarse SiC (HSc) exhibits more homogeneous and less porous microstructure. It was concluded that the decreasing of SiC content as a result of siliconization during the in-situ synthesis altered the oxidation mechanism of samples. As mentioned before, determined SiC volume ratio was lower for both samples compared with starting ratio and HSf has also lower SiC volume fraction. For a low SiC content, the amount of formed silica glass was not enough to fill the pores, cracks and grain boundaries and resulted lower oxidation resistance. Moreover, inhomogeneous distribution of SiC particles was also a reason for the more porous and less continuous SiO<sub>2</sub> layer in the HSf as well as SiC amount and particle size.

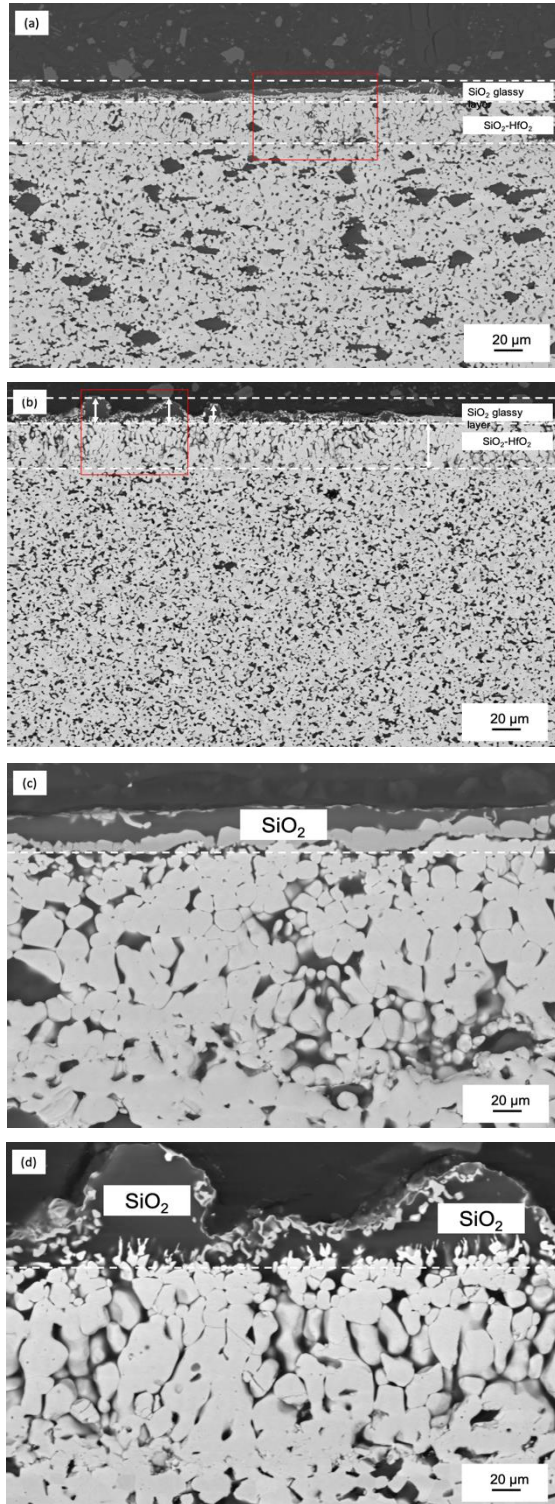


**Figure 6.** SEM (BSE) images of the polished cross-section surface after the oxidation test for 1h at 1650°C in the flowing dry air of a) HSc and b) HSf c) magnified view of red rectangular area of HSc and d) magnified view of red rectangular area of HSf samples.

Oxygen transport in grain boundaries was faster than grains, so intergranular SiC particles exhibit higher oxidation rate than intragranular SiC particles. This

caused the locally high SiO<sub>2</sub> formation on the oxide scales in regions with containing rich SiC as observed HSf. Quanli et al. [46] have also shown effect of SiC particle size on the oxidation behavior. According to their results, nano-SiC particles exhibits higher mass gain and faster oxidation in same oxidation conditions compared with the micro-SiC. So, obtained results were in agreement with observations.

The thickness of individual layers of oxide scales formed on HSc and HSf, as assessed by analyzing SEM images of cross sections were shown in Table 3. At least five measurements were taken for each sample. Comparison of the results in this table indicates that SiC depleted layers containing mixture of HfO<sub>2</sub> and SiO<sub>2</sub> have almost similar thickness for both samples, while the SiO<sub>2</sub>-rich top layer of HSf was approximately two times thicker than the layer of HSc. As a consequence of this result, a faster silica-rich layer on the surface of the oxidized

**Table 3.** Thicknesses of the layers within the oxide scales formed on HSc1950 and HSf1950, subjected to exposure at 1650°C for 1h.

Sample Name	SiC-depleted layer (µm)	SiO <sub>2</sub> rich layer (µm)
HSc	24.57 ± 6.48	5.19 ± 1.62
HSf	24.39 ± 3.52	10.06 ± 5.17

HfB<sub>2</sub>-SiC composite was formed [11, 46, 48].

## 5. CONCLUSIONS

Different from the relevant literature, fabrication of HfB<sub>2</sub>-SiC composites was achieved by using HfO<sub>2</sub>, B, and SiC as starting powders by SPS. Effect of SiC particles size on microstructural, mechanical and oxidation properties was extensively investigated. Results revealed that denser microstructure, higher hardness and fracture toughness were obtained by using fine SiC. The primary toughening mechanism was found to be crack deflection for composite containing fine SiC. Unlike mechanical properties, composite containing coarse SiC was more resistant to oxidation at the same oxidation conditions despite formed higher grain size. Both samples exhibited similar oxidation scales on the cross section of oxidized samples, fine SiC added composite was more susceptible to damage contrary to literature. It was found that reduction of SiC amount due to siliconization and non-uniform distribution of SiC particles was caused to detrimental effect on the microstructures.

## ACKNOWLEDGEMENT

This study was supported by Anadolu University Research Fund with Grant no: 1505F506.



**DECLARATION OF ETHICAL STANDARDS**

The author(s) of this article declare that the materials and methods used in this study do not require ethical committee permission and/or legal-special permission.

**AUTHORS' CONTRIBUTIONS**

**Kübra GÜRCAN:** Performed the experiments and wrote the manuscript.

**Cevat BORA DERİN:** Analyse the results.

**Erhan AYAS:** Analyse the results.

**CONFLICT OF INTEREST**

There is no conflict of interest in this study.

**REFERENCES**

- [1] Levine R.S., Opila E., Halbig M., D Kiser J., Singh M., Salem A., "Evaluation of Ultra-High Temperature Ceramics for Aero Propulsion Use", *Journal of the European Ceramic Society*, 22: 2757-2767,(2002).
- [2] Fahrenholtz W. G., Hilmas G. E., Talmy I. G., Zaykoski J. A., "Refractory Diborides of Zirconium and Hafnium", *Journal of the American Ceramic Society*, 90:1347-1364,(2007).
- [3] Akin I., Goller G., "Spark Plasma Sintering of Zirconia-Toughened Alumina Composites and Ultra-High Temperature Ceramics Reinforced with Carbon Nanotubes", "Research and Innovation in Carbon Nanotube-Based Composites", (2015).
- [4] Ni D.W., Zhang G.J., Kan Y.M., Wang P.L., "Synthesis of Monodispersed Fine Hafnium Diboride Powders Using Carbo/Borothermal Reduction of Hafnium Dioxide", *Journal of the American Ceramic Society*, 91:2709-2712,(2008).
- [5] Wang H., Lee S. H., Kim H. D., Oh H. C., "Synthesis of Ultrafine Hafnium Diboride Powders Using Solution-Based Processing and Spark Plasma Sintering", *International Journal of Applied Ceramic Technology*, 11,(2014).
- [6] Brochu M., Gauntt B., Zimmerly T., Ayala A., Loehman R., "Fabrication of UHTCs by Conversion of Dynamically Consolidated Zr+B and Hf+B Powder Mixtures", *Journal of the American Ceramic Society*, 91:2815-2822,(2008).
- [7] Ni D.-W., Zhang G.-J., Kan Y.-M., Wang P.-L., "Hot Pressed HfB<sub>2</sub> and HfB<sub>2</sub>-20vol%SiC Ceramics Based on HfB<sub>2</sub> Powder Synthesized by Borothermal Reduction of HfO<sub>2</sub>", *International Journal of Applied Ceramic Technology*, 7:830-836,(2010).
- [8] Blum Y. D., Marschall J., Hui D., Adair B., Vestel M., "Hafnium Reactivity with Boron and Carbon Sources Under Non-Self-Propagating High-Temperature Synthesis Conditions", *Journal of the American Ceramic Society*, 91:1481-1488,(2008).
- [9] Zou J., Zhang G.-J., Kan Y.-M., Ohji T., "Pressureless sintering mechanisms and mechanical properties of hafnium diboride ceramics with pre-sintering heat treatment", *Scripta Materialia*, 62:159-162,(2010).
- [10] Parthasarathy T. A., Rapp R. A., Opeka M., Kerans R. J., "A model for the oxidation of ZrB<sub>2</sub>, HfB<sub>2</sub> and TiB<sub>2</sub>", *Acta Materialia*, 55:5999-6010,(2007).
- [11] Monteverde F., Bellosi A., "The resistance to oxidation of an HfB<sub>2</sub>-SiC composite", *Journal of the European Ceramic Society*, 25:1025-1031,(2005).
- [12] Monteverde F., "Ultra-high temperature HfB<sub>2</sub>-SiC ceramics consolidated by hot-pressing and spark plasma sintering", *Journal of Alloys and Compounds*, 428:197-205,(2007).
- [13] Fahrenholtz W. G., "Thermodynamic Analysis of ZrB<sub>2</sub>-SiC Oxidation: Formation of a SiC-Depleted Region", *Journal of the American Ceramic Society*, 90:143-148,(2007).
- [14] Monteverde F., Scatteia L., "Resistance to Thermal Shock and to Oxidation of Metal Diborides-SiC Ceramics for Aerospace Application", *Journal of the American Ceramic Society*, 90:1130-1138,(2007).
- [15] Mallik M., Ray K. K., Mitra R., "Oxidation behavior of hot pressed ZrB<sub>2</sub>-SiC and HfB<sub>2</sub>-SiC composites", *Journal of the European Ceramic Society*, 31: 199-215,(2011).
- [16] Carney C. M., Key T. S., "Comparison of the Oxidation Protection of HfB<sub>2</sub> Based Ultra-High Temperature Ceramics by the Addition of SiC or MoSi<sub>2</sub>", *Ceramic Engineering and Science Proceedings*, 35:261-273,(2014).
- [17] Monteverde F., Melandri C., Guicciardi S., "Microstructure and mechanical properties of an HfB<sub>2</sub>+30vol.% SiC composite consolidated by spark plasma sintering", *Materials Chemistry and Physics*, 100:513-519,(2006).
- [18] Quach D. V., Groza J. R., Zavaliangos A., Anselmi-Tamburini U., Fundamentals and applications of field/current assisted sintering, "Sintering of Advanced Materials", Woodhead Publishing, (2010).
- [19] Anselmi-Tamburini U., Kodera Y., Gasch M., Unuvar C., Munir Z. A., Ohyanagi M., Johnson S. M., "Synthesis and characterization of dense ultra-high temperature thermal protection materials produced by field activation through spark plasma sintering (SPS): I. Hafnium Diboride", *Journal of Materials Science*, 41:3097-3104,(2006).
- [20] Wang H., Lee S. H., Kim H. D., Chamberlain A., "Nano-Hafnium Diboride Powders Synthesized Using a Spark Plasma Sintering Apparatus", *Journal of the American Ceramic Society*, 95, (2012).
- [21] Yuan H., Li J., Shen Q., Zhang L., "In situ synthesis and sintering of ZrB<sub>2</sub> porous ceramics by the spark plasma sintering-reactive synthesis (SPS-RS) method", *International Journal of Refractory Metals and Hard Materials*, 34:3-7,(2012).
- [22] Wang H., Lee S.-H., Feng L., "HfB<sub>2</sub>-SiC composite prepared by reactive spark plasma sintering", *Ceramics International*, 40:11009-11013,(2014).
- [23] Wu W.W., Estili M., Nishimura T., Zhang G.J., Sakka Y., "Machinable ZrB<sub>2</sub>-SiC-BN composites fabricated by reactive spark plasma sintering", *Materials Science and Engineering: A*, 582:41-46,(2013).
- [24] Xiang M., Gu J., Ji W., Xie J., Wang W., Xiong Y., Fu Z., "Reactive spark plasma sintering and mechanical properties of ZrB<sub>2</sub>-SiC-ZrC composites from ZrC-B<sub>4</sub>C-Si system", *Ceramics International*, 44:8417-8422,(2018).

- [25] Shahedi Asl M., Nayebi B., Ahmadi Z., Parvizi S., Shokouhimehr M., "A novel ZrB<sub>2</sub>-VB<sub>2</sub>-ZrC composite fabricated by reactive spark plasma sintering", *Materials Science and Engineering: A*, 731:131-139,(2018).
- [26] Monteverde F., "Progress in the fabrication of ultra-high-temperature ceramics: "in situ" synthesis, microstructure and properties of a reactive hot-pressed HfB<sub>2</sub>-SiC composite", *Composites Science and Technology*, 65:1869-1879,(2005).
- [27] Jun Lee S., Son Kang E. U. L., Su Baek S., Kim D. K., "Reactive Hot Pressing and Oxidation Behavior of Hf-Based Ultra-High-Temperature Ceramics", *Surface Review and Letters (SRL)*, 17:215-221,(2010).
- [28] Bale C. W., Bélisle E., Chartrand P., Deckerov S. A., Eriksson G., Gheribi A. E., Hack K., Jung I. H., Kang Y. B., Melançon J., Pelton A. D., Petersen S., Robelin C., Sangster J., Spencer P., Van Ende M. A., "FactSage thermochemical software and databases, 2010–2016", *Calphad*, 54:35-53,(2016).
- [29] Evans A. G., Charles E. A., "Fracture Toughness Determinations by Indentation", *Journal of the American Ceramic Society*, 59:371-372,(1976).
- [30] Munir Z. A., Anselmi-Tamburini U., Ohyanagi M., "The effect of electric field and pressure on the synthesis and consolidation of materials: A review of the spark plasma sintering method", *Journal of Materials Science*, 41:763-777,(2006).
- [31] Angerer P., Artner W., Neubauer E., Yu L. G., Khor K. A., "Residual stress in spark-plasma-sintered and hot-pressed tantalum samples determined by X-ray diffraction methods", *International Journal of Refractory Metals and Hard Materials*, 26:312-317,(2008).
- [32] Wang H., Fan B., Feng L., Chen D., Lu H., Xu H., Wang C.-A., Zhang R., "The fabrication and mechanical properties of SiC/ZrB<sub>2</sub> laminated ceramic composite prepared by spark plasma sintering", *Ceramics International*, 38:5015-5022,(2012).
- [33] Telle R., Sigl L. S., Takagi K., "Boride-Based Hard Materials", "Handbook of Ceramic Hard Materials", (2000).
- [34] Ran S., Van der Biest O., Vleugels J., "In situ platelet-toughened TiB<sub>2</sub>-SiC composites prepared by reactive pulsed electric current sintering", *Scripta Materialia*, 64:1145-1148,(2011).
- [35] Rangaraj L., Divakar C., Jayaram V., "Fabrication and mechanisms of densification of ZrB<sub>2</sub>-based ultra high temperature ceramics by reactive hot pressing", *Journal of the European Ceramic Society*, 30:129-138,(2010).
- [36] Rangaraj L., Suresha S., Canchi D., Jayaram V., "Low-Temperature Processing of ZrB<sub>2</sub>-ZrC Composites by Reactive Hot Pressing", *Metallurgical and Materials Transactions A: Physical Metallurgy and Materials Science*, 39:1496-1505,(2008).
- [37] Sokolov P. S., Mukhanov V. A., Chauveau T., Solozhenko V. L., "On melting of silicon carbide under pressure", *Journal of Superhard Materials*, 34:339-341,(2012).
- [38] Davis S. G., Anthrop D. F., Searcy A. W., "Vapor Pressure of Silicon and the Dissociation Pressure of Silicon Carbide", *The Journal of Chemical Physics*, 34:659-664,(1961).
- [39] Yudin B. F., Borisov V. G., "Thermodynamic analysis of dissociative volatilization of silicon carbide", *Refractories*, 8:499-504,(1967).
- [40] Takeuchi T., Takahashi M., Ado K., Tamari N., Ichikawa K., Miyamoto S., Kawahara M., Tabuchi M., Kageyama H., "Rapid Preparation of Lead Titanate Sputtering Target Using Spark-Plasma Sintering", *Journal of the American Ceramic Society*, 84:2521-2525,(2004).
- [41] Özerdem E., Ayas E., "Fabrication and microstructural stability of spark plasma sintered Al<sub>2</sub>O<sub>3</sub>/Er<sub>3</sub>Al<sub>5</sub>O<sub>12</sub> eutectic", *Ceramics International*, 41:12869-12877,(2015).
- [42] Gürcan K., Ayas E., "In-situ synthesis and densification of HfB<sub>2</sub> ceramics by the spark plasma sintering technique", *Ceramics International*, 43:3547-3555,(2017).
- [43] Zhu S., Fahrenholtz W. G., Hilmas G. E., "Influence of silicon carbide particle size on the microstructure and mechanical properties of zirconium diboride-silicon carbide ceramics", *Journal of the European Ceramic Society*, 27:2077-2083,(2007).
- [44] Zapata-Solvas E., Jayaseelan D. D., Lin H. T., Brown P., Lee W. E., "Mechanical properties of ZrB<sub>2</sub>- and HfB<sub>2</sub>-based ultra-high temperature ceramics fabricated by spark plasma sintering", *Journal of the European Ceramic Society*, 33:1373-1386,(2013).
- [45] Swanson P. L., Fairbanks C. J., Lawn B. R., Mai Y.-W., Hockey B. J., "Crack-Interface Grain Bridging as a Fracture Resistance I, Mechanism in Ceramics: I, Experimental Study on Alumina", *Journal of the American Ceramic Society*, 70:279-289,(1987).
- [46] Quanli J., Haijun Z., Suping L., Xiaolin J., "Effect of particle size on oxidation of silicon carbide powders", *Ceramics International*, 33:309-313,(2007).
- [47] Hu P., Guolin W., Wang Z., "Oxidation mechanism and resistance of ZrB<sub>2</sub>-SiC composites", *Corrosion Science*, 51:2724-2732,(2009).
- [48] Monteverde F., "Beneficial effects of an ultra-fine  $\alpha$ -SiC incorporation on the sinterability and mechanical properties of ZrB<sub>2</sub>", *Applied Physics A*, 82:329-337,(2006).